# Author's Accepted Manuscript

Halocarbons associated with Arctic sea ice

Helen M. Atkinson, Claire Hughes, Marvin J. Shaw, Howard K. Roscoe, Lucy J. Carpenter, Peter S. Liss

Cite this article as: Helen M. Atkinson, Claire Hughes, Marvin J. Shaw, Howard K. Roscoe, Lucy J. Carpenter, Peter S. Liss, Halocarbons associated with Arctic sea ice, *Deep-Sea Research I*, http://dx.doi.org/10.1016/j.dsr.2014.05.012

**Halocarbons Associated with Arctic Sea Ice**

Helen M. Atkinson[a,b], Claire Hughes[b,d], Marvin J. Shaw[c], Howard K. Roscoe[a]*, Lucy J. Carpenter[c], Peter S. Liss[b],

[a]British Antarctic Survey, High Cross, Madingley Road, Cambridge, CB3 0ET, UK.

[b]University of East Anglia, Norwich, NR4 7TJ, UK.

[c]University of York, Heslington, York, YO10 5DD, UK.

[d]Now at University of York, Heslington, York, YO10 5DD, UK.

*Corresponding author   22 May 2014

**Abstract**

Short-lived halocarbons were measured in Arctic sea-ice brine, seawater and air above the Greenland and Norwegian seas (~81°N, 2 to 5°E) in mid-summer, from a melting ice floe at the edge of the ice pack.  In the ice floe, concentrations of $C_2H_5I$, $2-C_3H_7I$ and $CH_2Br_2$ showed significant enhancement in the sea ice brine, of average factors of 1.7, 1.4 and 2.5 times respectively, compared to the water underneath and after normalising to brine volume. Concentrations of mono-iodocarbons in air are the highest ever reported, and our calculations suggest increased fluxes of halocarbons to the atmosphere may result from their sea-ice enhancement.  Some halocarbons were also measured in ice of the sub-Arctic in Hudson Bay (~55°N, 77°W) in early spring, ice that was thicker, colder and less porous than the Arctic ice in summer, and in which the halocarbons were concentrated to values over 10 times larger than in the Arctic ice when normalised to brine volume.  Concentrations in the Arctic ice were similar to those in Antarctic sea ice that was similarly warm and porous.  As climate warms and Arctic sea ice becomes more like that of the Antarctic, our results lead us to expect the production of iodocarbons and so of reactive iodine gases to increase.

## 1.  Introduction

There has been much speculation about sources of reactive halogens in the polar troposphere.  The presence of high concentrations of both iodine and bromine monoxide (IO and BrO) over Antarctica and its sea ice [*Saiz-Lopez et al.* 2007, *Schoenhardt et al.* 2008] suggests an iodine-selective mechanism, as the sum of iodide plus iodate is 1000 times less abundant than bromide in seawater.  Although IO has been measured above sub-Arctic sea ice at amounts of up to 4 pptv [*Mahajan et al.* 2010], this is less than a quarter the Antarctic concentrations.

Iodine and bromine radicals in the atmosphere form oxides via ozone depletion mechanisms [*Chameides and Davis* 1980, *Davis et al.* 1996] and the oxidising capacity may be altered by reactions involving $HO_x$ (OH + $HO_2$) and $NO_x$ (NO +$NO_2$) [*Davis et al.* 1996].  Iodine compounds are also important because they form higher oxides which can form new particles [*O'Dowd et al.* 2002]; if they grow to the size of cloud condensation nuclei they may impact climate via increased scattering of sunlight [*Slingo*, 1990].  Hence understanding the processes which control the volatilisation and release of halogens in polar regions is important for regional chemistry and climate.

Diatoms are known to live in sea ice brine channels [*Garrison & Buck* 1989], and the production of halocarbons by diatoms is well established [*Sturges et al.* 1992, *Tokarczyk & Moore* 1994], via enzymes active in the metabolism of the cell [*Manley* 2002, *Moore et al.* 1996].

Previous halocarbon measurements in the Arctic are summarised in Supplementary Tables S1 and S2.  Enhanced concentrations have been measured in sea ice brine and ice covered water.  In Hudson Bay, halocarbons were observed in air in the absence of open leads [*Carpenter et al.* 2005]; for some iodocarbons they were the highest atmospheric concentrations ever recorded. The authors proposed an abiotic mechanism for their production via the reaction of HOI with humic material in the quasi-liquid layer on the surface of sea ice.

Halocarbon measurements have so far been unable to account for the iodine atom flux necessary to maintain the high concentrations of IO found in Antarctica [e.g. *Carpenter et al.* 2007], but inorganic iodine compounds are implicated [*Atkinson et al.* 2012].  Until recently, there was a large difference in the sea ice of the Arctic and Antarctic, the Arctic being thicker, colder, and more likely to be multi-year  [*Arrigo and Thomas*, 2004].  As the planet warms and Arctic sea ice thins and retreats, the ice is becoming ever more like that of the Antarctic, which has implications for ice biota and the release of compounds produced.

Here, we present halocarbon measurements from air, sea ice brine and underlying seawater, from a ship moored against an ice floe while it drifted south and partly melted, and from the nearby open ocean – for the first time in the pack ice of the Arctic Ocean.  We estimate the fluxes and loss processes, discuss production pathways and the effect of ice conditions.  We also compare the results to those from very different sub-Arctic ice in early spring, and to earlier results in Antarctic sea ice with similar properties to those in the Arctic summer.
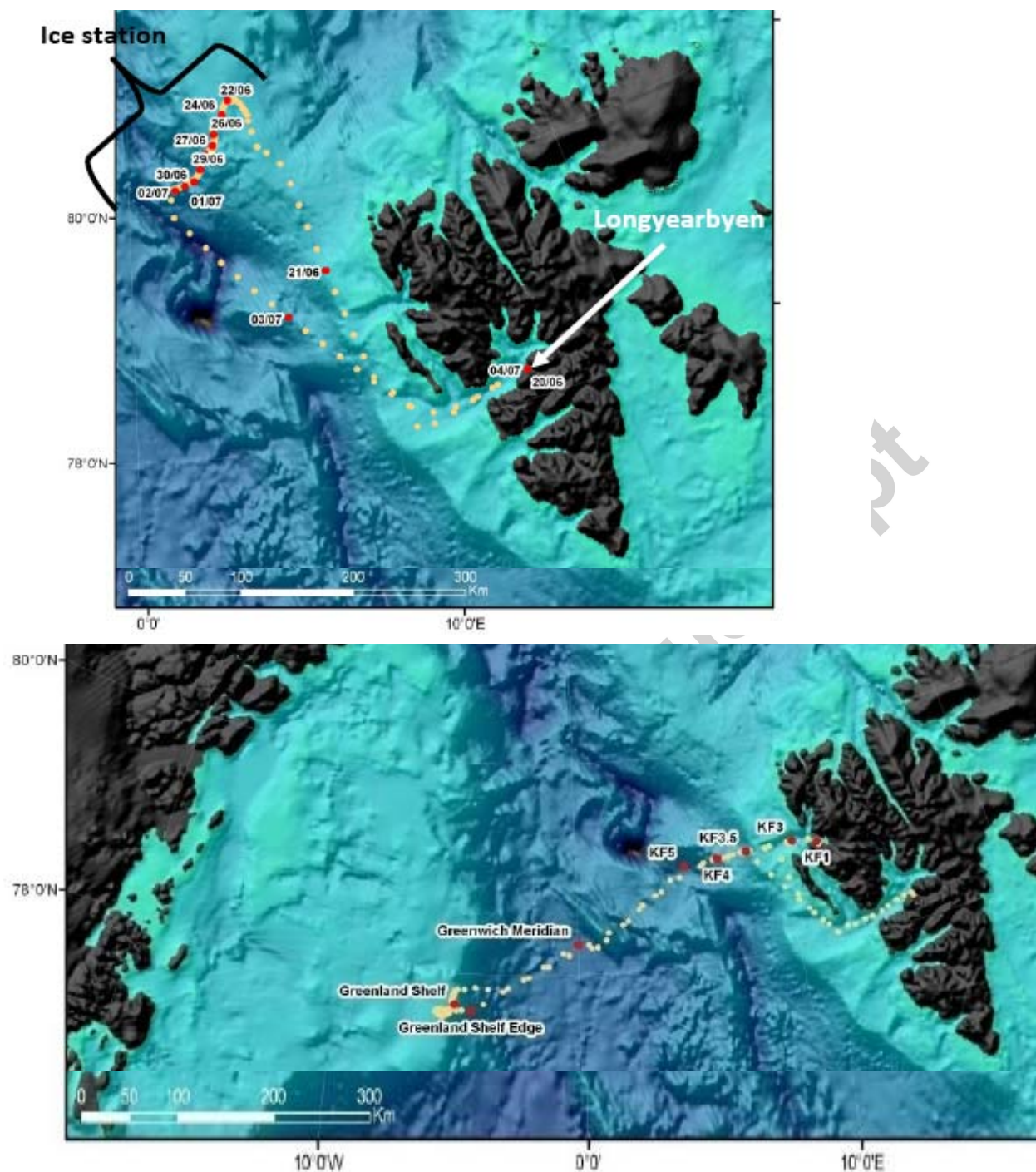
**2. Materials and Methods**



Fig. 1. Cruise path of JR219: upper panel – 20 June to 3 July 2010; lower panel – 3 to 13 July 2010.

Measurements were made from 18 June to 10 July 2010 from the ice-strengthened RRS James Clark Ross (Figure 1). The ship sailed from Longyearbyen, Svalbard (78.2°N, 15.6°E) into pack ice of average ice thickness 1 m. It moored against an ice floe of about 1.3 km diameter at 80.9°N, 5.4°E on 21 June 2010 where an ice station was set up. Ice cores were made, sea ice brine collected, and air and water samples were taken regularly, until 1 July 2010, by which time the floe had drifted to 80.2°N, 2.9°E. Later, air and water samples were taken from Longyearbyen to pack ice near Greenland at 77.7°N, 5.6°W. Water samples were also taken from the open ocean approaching, underneath and within the sea ice. Temperature-salinity profiles and biological data were used to interpret the measurements.

**2.1. Sample collection – sea ice brine from cores**
It is challenging to collect brine from sea ice without escape of volatile trace gases – as a core is lifted from the ice, brine immediately begins to drain. A 9 cm diameter SIPRE corer (Mark II coring system from Kovacs Enterprises

Inc.) was used to make a core in the sea ice, and the corer was lifted from the ice and immediately placed into a small plastic bucket whose sides contacted the corer.  To collect this so-called 'drainage brine', after about 30 s the corer was removed from the bucket and the brine in the bucket was sucked into a 100 ml gas-tight syringe via a piece of Tygon tubing placed at the bottom of the bucket to prevent collection of brine exposed to the atmosphere. The syringe was filled except where limited by the volume of brine which drained from the ice, which only occured in the top-most sections.

At each location and date, several cores were made nearby, to progressively deeper depths (10 cm, 20 cm, etc) in order that a vertical profile of halocarbon concentrations through the ice could be deduced.  A problem then arises because the brine includes the contribution from the entire length of the core, so in figures below showing profiles in cores, each point represents the brine from the entire core, and the depth shown is the full depth of the core.

We also collected brine from each hole in the sea ice, but this hole brine was unreliable as a measure of sea ice brine – see Supplementary Section S1.

### 2.2. Water and air samples

**Air samples** were collected from the deck of the ship facing into the wind by drawing air through a Markes sorbent tube at a rate of < 100 ml min$^{-1}$ with a gas-tight syringe.  1 litre of air was sampled.  Triplicate samples were collected, on 19 days.

**CTD water samples** were collected with Niskin bottles used for routine conductivity/temperature/depth (CTD) measurements, from the surface, and from the depth of chlorophyll maximum (DCM) which ranged from 14 to 57 m. Water was sampled with a filled 100 ml gas-tight syringe via Tygon tubing attached to the bottom valve of the Niskin bottle.  Samples were taken when time permitted from 20 June to 3 July, and daily from 3 July.  Measurements were made in ice-covered waters on 25 and 28 June, and on 8 and 9 July.

**Under-ice water samples** were collected from a dedicated water sampling hole, away from other activities at the ice station, via a 2.5 m Teflon tube from the ice-water interface to a plastic valve.  100 ml gas-tight syringes were used to take triplicate samples daily.

**Under-ice water samples from the dive team** were collected as depicted in Figure 2: (A) under ice water; (B) water / brine collected by drawing water into a gas-tight syringe held against the underside of ice that was visibly discoloured by diatoms (the lighter brown patches in Figure 2) - algae could be seen entering the syringe during sample collection; and (C) large aggregates of dead and decaying plankton which collect following brine channel drainage (Figure 2 insert), placed into the 100 ml syringe with the surrounding seawater.

In total 23 water samples from CTD bottles, 9 water samples from the hole in the ice floe, 18 brine samples from 3 ice cores and 9 samples collected by the dive team were analysed.  Most brine samples were made in duplicate, except where limited by sample volume in the shallowest cores.  CTD water samples, under-ice water and air samples were made in triplicate, except for the CTD profile of 28 June, when only duplicate samples were made. After collection, samples were stored in the dark at 4°C for a maximum duration of 6 hours before analysis.

### 2.3. Sample preparation and analysis

**Brine and water samples** were filtered through 47 µm Whatman GF/F filters directly into a glass purge tube (taking care to avoid introducing bubbles), where halocarbons were extracted by purging for 10 min with oxygen-free nitrogen at 95 ml min$^{-1}$.  We checked that the filters did not cause any loss of halocarbons.  Extraction efficiencies were measured and applied.  Particles were removed from the purge-gas stream using glass wool, followed by a counterflow Nafion dryer to remove water; the glass wool was the same material as the purge tube, on which no halocarbons are lost.  Halocarbons were then trapped and stored on Markes three-bed solid sorbent tubes containing Tenax, Carbograph and Carboxen held at 0°C by a Peltier cooler.  The filters were wrapped in aluminium foil and stored at -80°C on the ship for Chl *a* analysis in UK.

**Halocarbon analysis** was carried out on the ship, immediately after filtration.  The sorbent tubes were removed from the Peltier cooler by hand and transferred to a Markes Unity thermal desorption unit and UltrA autosampler connected to an Agilent gas chromatograph–mass spectrometer (GCMS).  The GC was fitted with a 60-m capillary column (DB-VRX, J&W) and the MS operated with an electron ionisation detector in single ion mode.  Following desorption, compounds were refocused on a cold trap at -10°C: whilst trapping efficiencies are larger with a liquid nitrogen trap, an adsorbent tube cooled to -10°C by a Peltier has been successfully used for fieldwork where liquid

nitrogen is difficult to organise (Hughes et al. 2008, Hughes et al. 2009). Trapping efficiencies were measured and applied to the data. The cold trap was then heated to 290°C to transfer the compounds into the GC column using helium at a flow rate of 2 ml min$^{-1}$ (further technical details of coolers and heaters can be found in the relevant Markes manual). The oven was held at 36°C for 5 min at the start of the GC run, then heated to 200°C at 20°C min$^{-1}$, held at 200°C for 2 min and then heated to 240°C at 40°C min$^{-1}$. Table 1 gives retention times and limits of detection of the 8 halocarbons measured. A calibration was carried out at the start and end of the campaign; instrument sensitivity during the campaign was monitored by injecting every sample with a known concentration of deuterated 1-iodopropane and deuterated methyl iodide dissolved in methanol, which was checked for contamination at regular intervals. $R^2$ values for all calibration curves were above 0.98. Liquid standards were used for the calibration, injecting known concentrations of standards (Sigma) dissolved in methanol (Fisher HPLC grade) into pre-purged seawater. The standards were prepared in UK, dissolved in methanol, and stored at -20°C, in amber glass vials with Thames Restec mini-inert valve caps to prevent evaporation. The details of preparation and storage of standards were developed in at UEA for earlier field campaigns, where their stability had been checked by comparing to newly prepared ones after the campaign.

To extrapolate from water concentrations to mixing ratios in air, we used extraction efficiencies of the halocarbons in water, determined from previous laboratory measurements to be CH3I = 1; C2H5I = 1; CHBr3 = 0.5; CH2ICl = 0.6; 2-C3H7I = 0.6; CH2I2 = 0.4; CH2IBr = 0.6; CHBr2Cl = 0.6; 1-C3H7I = 0.6; CH2Br2 = 0.6. Measurement precision, determined by repeat analysis of known concentrations of halocarbons in water, was between 0.5% and 8.0%.
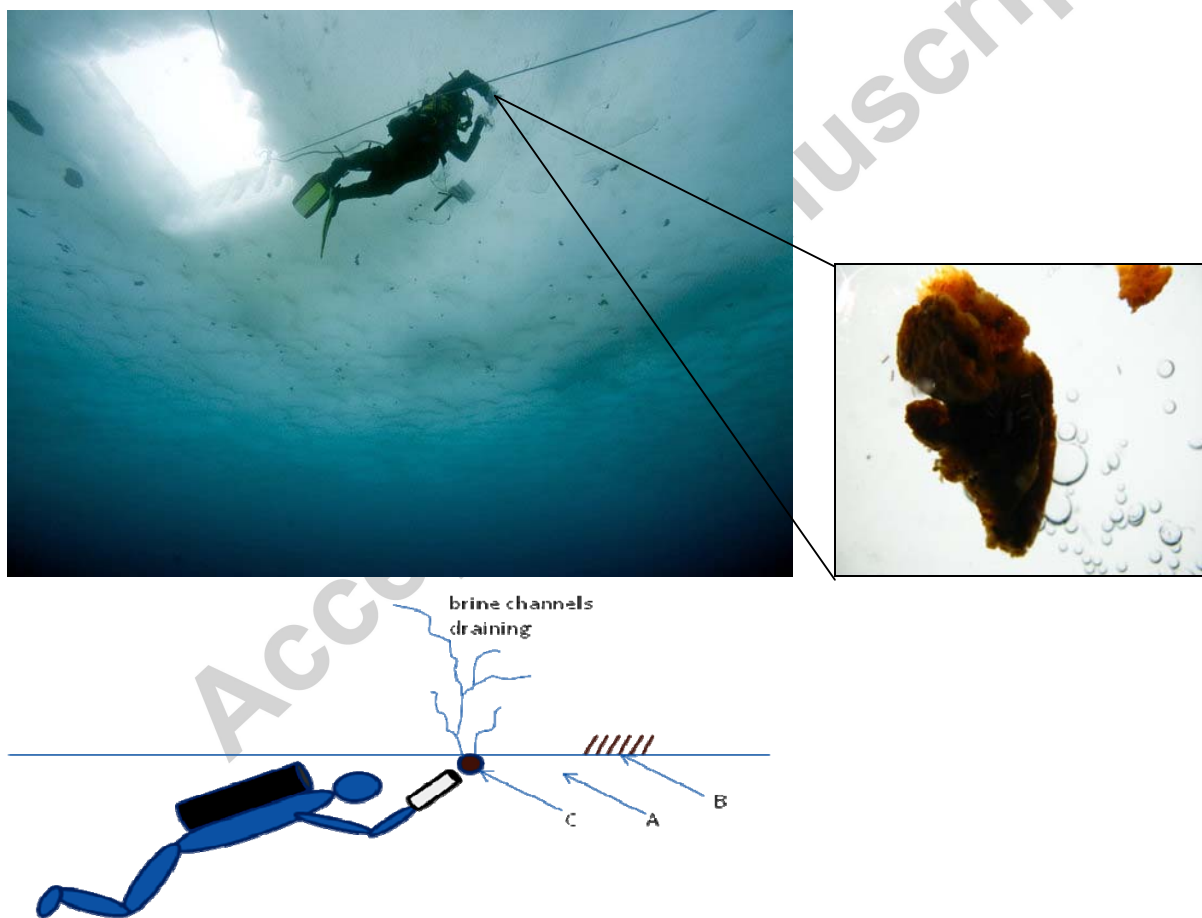


Fig. 2. Sample collection by the dive team, see text for details. Photos courtesy Heiko Moossen.

Chl *a* was measured in brine and under-ice water by a Turner AU-10 fluorometer following extraction overnight in darkness at 4°C, in 10 ml of 90% acetone buffered with MgCO$_3$. Concentrations were corrected for interference from phaeophytin *a* by measuring fluorescence before and after acidification with 8% HCl, and calibrated using a standard (1 mg chlorophyll *a* from *Anacystis nidulans*, diluted in 90% buffered acetone, Sigma-Aldrich) whose concentration had been determined spectrophotometrically. Chl *a* in CTD water was measured by a Chelsea Aqua 3 fluorometer on board the sampling rosette, but was not calibrated so the results should be taken as relative values only.

---

Table 1. Halocarbons analysed by GCMS, showing mass/charge ratio (m/z), limit of detection (LoD) in pM, and retention times (RT) in minutes.  The LoD at the start of the campaign is given, in most cases it improved with time.

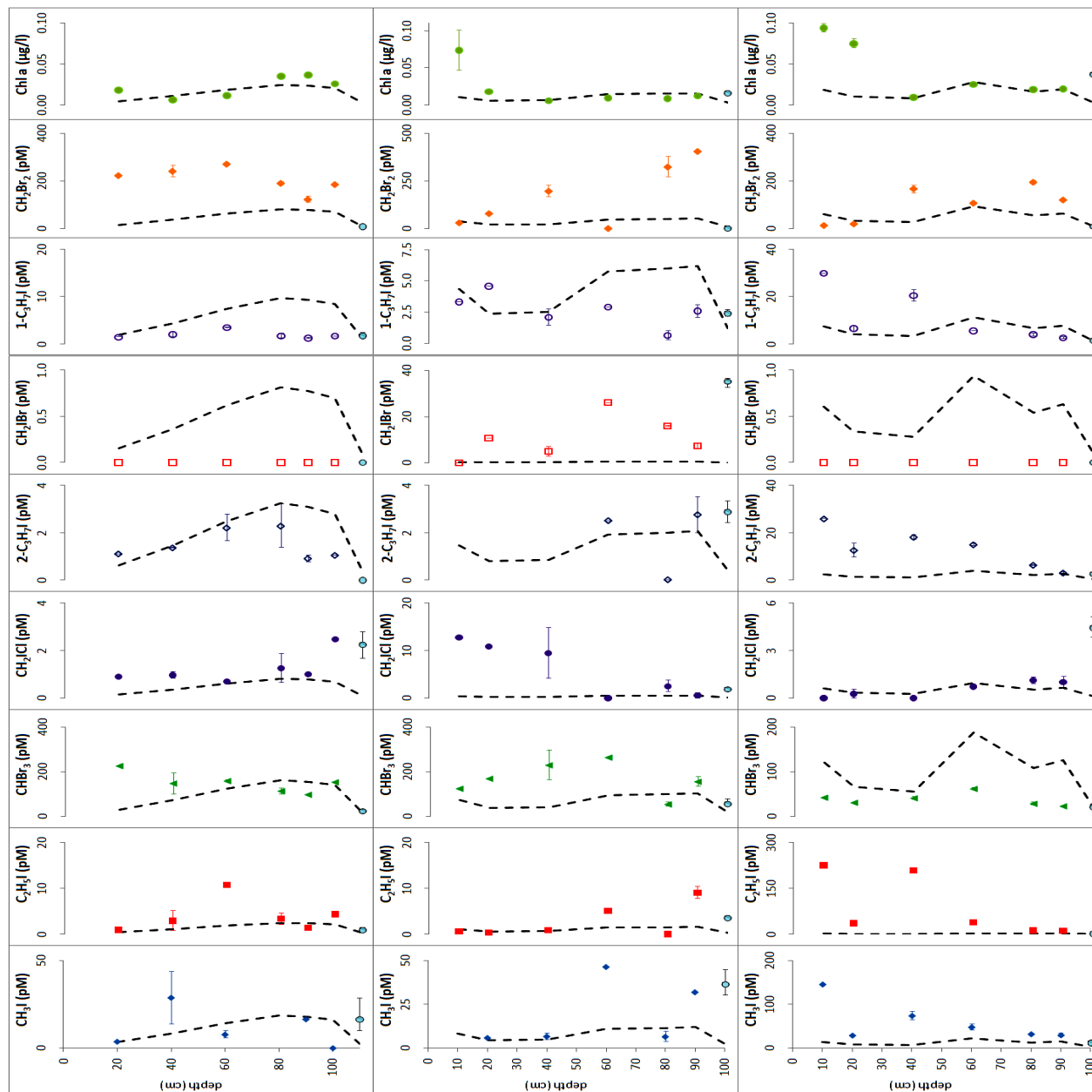|  | $CH_3I$ | $C_2H_5I$ | $CHBr_3$ | $CH_2ICl$ | $2-C_3H_7I$ | $CH_2IBr$ | $1-C_3H_7I$ | $CH_2Br_2$ |
|---|---|---|---|---|---|---|---|---|
| m/z | 142 | 156 | 173 | 176 | 170 | 222 | 170 | 174 |
| LoD | 1.6 | 0.09 | 1.5 | 1.2 | 0.5 | 1.1 | 1.1 | 0.06 |
| RT | 6.74 | 8.7 | 12.8 | 10.5 | 9.8 | 11.8 | 10.5 | 10.1 |

---



Fig. 3.  Halocarbons in sea ice brine that drained from cores, each set of cores being made nearby and to the indicated depth, in an ice floe in the Arctic summer approximately 1 m thick.  Sets of cores were made on 25 June (left), 27 June (centre) and 29 June (right).  The lowest depth on each graph is the concentration in underlying seawater. Average and range of duplicate samples are shown. The dashed line of each plot shows the expected concentration if open water values are divided by the brine volume (the ratio of brine to original sea water).

**Wind speed & direction, and temperature, salinity & Chl *a* at 6 m depth**, were from the ship's logger (Figure S1).

**Temperature** of the ice was measured with a handheld temperature probe after drilling small holes in the side of the core with a cordless drill.  **Salinity** of the bulk ice samples was measured after melting them using a Hach sensION5

ISFET conductivity meter with internal temperature correction, resolution 0.1 g l$^{-1}$, nominal accuracy 0.1 practical salinity units (psu). **Brine volume** of the ice was calculated from the temperature and salinity according to the empirical equations of Frankenstein and Garner [1967]:

$$V_b = S_i ((45.917 / |\theta|) + 0.930) \text{ when } -8.2 \le \theta \le 2.0°C \quad (1)$$
$$V_b = S_i ((43.975 / |\theta|) + 1.189) \text{ when } -22.9 \le \theta \le -8.2°C \quad (2)$$

where $V_b$ is brine volume (dimensionless proportion), $S_i$ is bulk salinity (psu) and $\theta$ is temperature (°C). Tests with salinity measurements of CTD water samples agreed with those by the CTD sampler within 0.7 psu.

## 2.4. The sub-Arctic in early spring

Methods for this earlier campaign are discussed in Supplementary Material S2. Briefly, the campaign in February and March 2008 took place on the east coast of Hudson Bay near Kuujjuarapik (55.3°N, 77.7°) at the sea ice edge, which was frozen apart from coastal leads some 100 to 1000 km away. Sea ice cores were taken with a different protocol because of the thicker and less saline ice. A similar but not identical GCMS system was used (Mahajan et al. 2010), with similar supporting measurements.

## 3. Results

The temperature of the ice ranged from -0.1 to -1.6°C (the melting point of older sea ice is higher than the freezing point of sea water due to it being less saline because brine has drained). Brine volume (the ratio of brine volume to that of the sea water from which it came) in the ice ranged from 11 to 51%, well above the 5% threshold for brine network connectivity [*Golden et al.*, 1998]. Chl *a* concentrations ranged from 0.006 to 0.09 µg l$^{-1}$ in the ice, 0.013 to 1.1 µg l$^{-1}$ in the water underneath, and up to 3.4 µg l$^{-1}$ at the DCM in waters in which the phytoplankton bloom was well underway. This last value is typical of productive Arctic waters [*Harrison and Cota,*1991]. The diatom communities in the ice and water were dominated by small pennate diatoms.

## 3.1 Halocarbons in sea ice brine

Vertical profiles of halocarbons throughout the sea-ice brine are shown in Figure 3. The concentrations that would be expected from the concentration effect are shown for comparison, calculated by scaling seawater concentrations by brine volume. Under-ice seawater concentrations were not used as these are likely to be influenced by nearby brine rejection and by emissions from under-ice algae. Instead, seawater from open areas close to the ice was used. Although this calculation has errors due to brine drainage and fresh water melt influx to the brine channels, it is useful to consider whether halocarbons are enhanced or reduced compared to that expected solely from passive transport. Where concentrations are larger than those expected by the concentration effect, in-situ production of halocarbons could be occurring, whereas loss processes may dominate when values are smaller. Chl *a* amounts are also shown in Figure 3 as an indication of diatom distribution in the ice.

The cores show a mixed pattern of some enhancement beyond the concentration effect, some depletion, and some with neither. These results suggest a complex system with different production and loss processes competing to influence halocarbon concentrations. Production by sea ice biota and photochemical reactions compete with uptake to the diatom particulates, consumption by bacteria, loss to the seawater below and gas exchange with the atmosphere, so the brine channels are not inert pathways.

Table 2 summarises our halocarbon measurements in sea ice brine, and compares them to previous measurements by others [*Fogelqvist and Tanhua* 1995] and to an earlier study by some of us [*Atkinson et al.* 2012] in Antarctic sea ice with similar properties. A different sampling technique was used by *Atkinson et al.* [2012], who sampled the bulk ice, with brine concentrations calculated by normalising to liquid water content.

## 3.2 Halocarbons in seawater

Results for seawater halocarbons are shown in Figures 4 and 5. The ice floe decreased in thickness by approximately 3 cm day$^{-1}$ (Gavin Turner, private communication). Whilst at the ice station, concentrations of some halocarbons had a tendency to increase for the first two days then decrease. This might be explained by ice melt plus water currents, as follows: on 22 June the water inlet was set to be level with the ice-water interface; as ice melts from below, the water sampled later was ever further from the interface; but any under-ice blooms would produce halocarbons – hence the peak in concentrations would occur a short distance from the ice. Exceptions (e.g. CH$_2$ICl, which steadily increases with time), suggest production by algae not associated with ice.
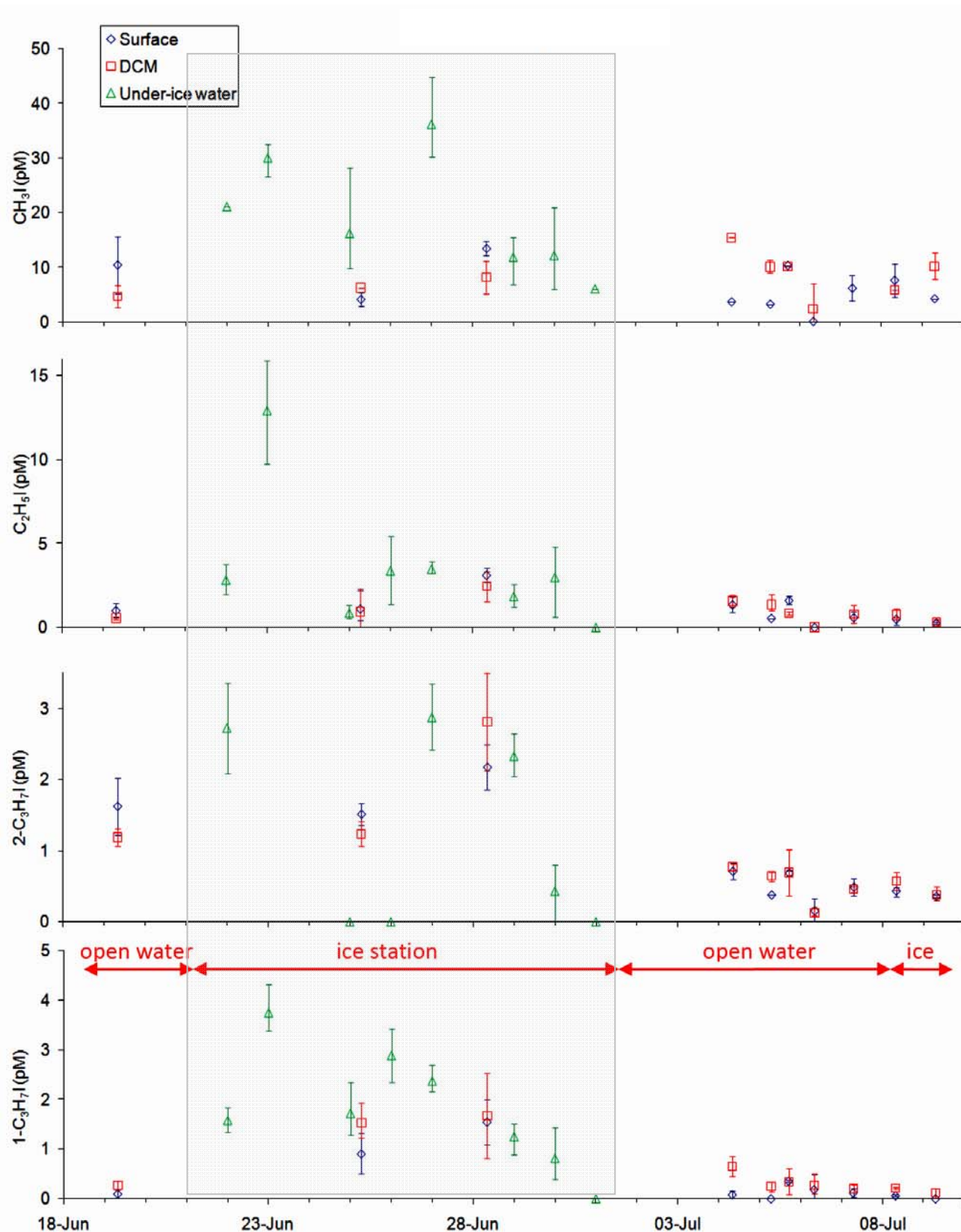
Fig. 4. Iodocarbon concentrations in water samples: by CTD within the top metre of the water column (Surface) and at the depth of chlorophyll maximum (DCM); and from underneath the sea ice when the ship was moored at the ice station (21 June to 1 July). On 8 and 9 July the ship was close to the pack ice east of Greenland. Note that both forms of $C_3H_7I$ have larger concentrations at the ice station (the grey shaded box), and that all under-ice concentrations are larger than those in open water or pack ice.
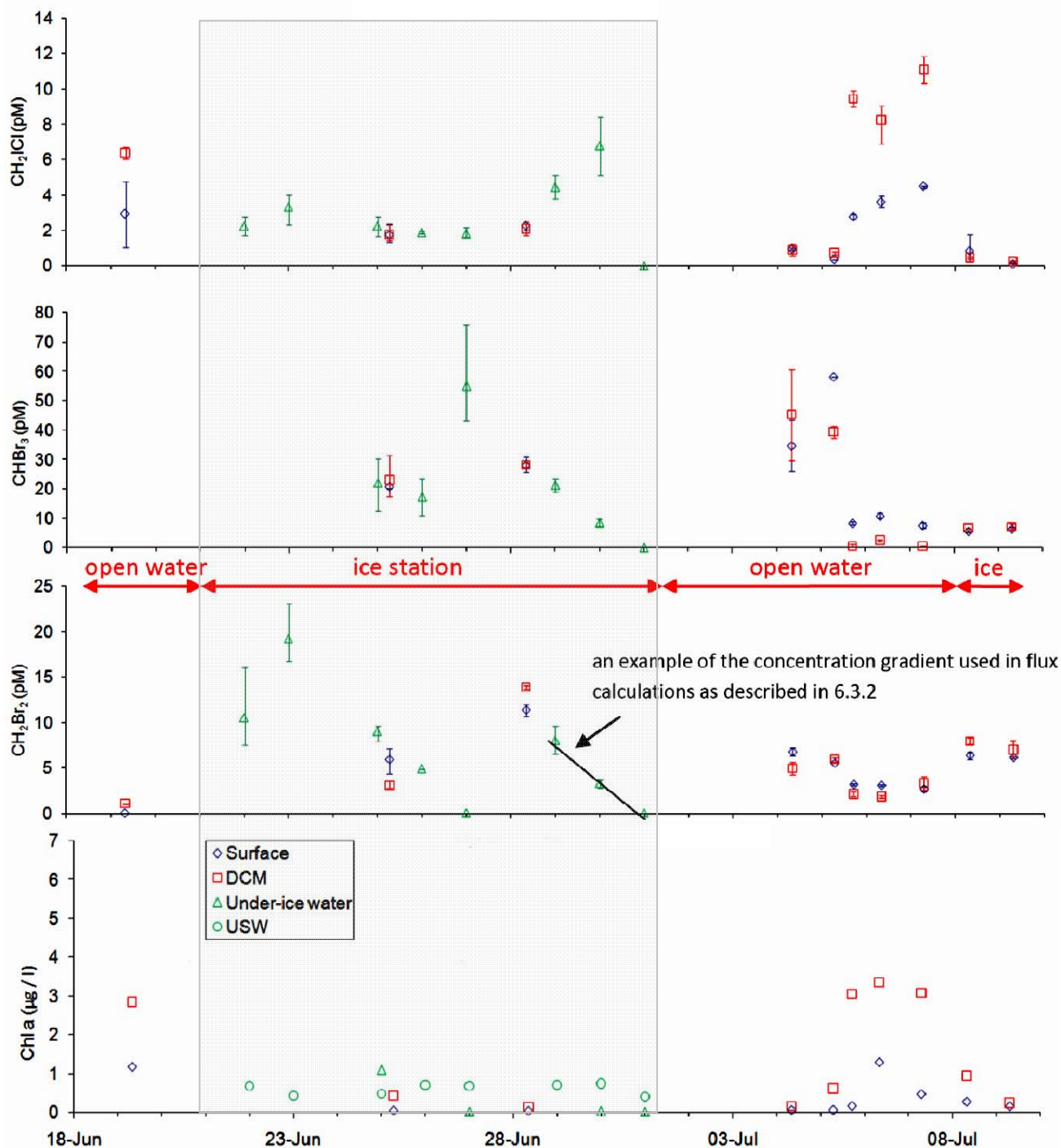
Fig. 5. As Figure 4 but for other halocarbons and Chl *a*, and including some Chl *a* samples from the ship's Underway Sea Water (USW) supply whilst at the ice station. $CH_2IBr$ was only measured above the LoD in one under-ice sample on 27 June (35 pM), and four CTD samples from 4 to 7 July (< 2.2 pM). In open water on 19 June and 4 to 7 July there is a clear difference in biological activity between the surface and the DCM, whereas in ice covered waters the concentrations are similar at the different depths and are smaller than in open water.

Away from the ice, iodocarbon concentrations were smaller (Figures 4 and 5), except $CH_2ICl$ which shows a significant increase at the DCM in open waters, again suggesting its production by algae not associated with ice. $CH_2ICl$ is also the only halocarbon that is highly correlated to biological activity: Chl *a* ($\mu g \ l^{-1}$) = 0.32 $CH_2ICl$ (pM) – 0.07 ($R^2$=0.8 with 28 points). Concentrations of all other halocarbons are higher in sea ice brine and in ice covered waters, consistent with production by ice diatoms [e.g. *Moore et al.* 1996] or by other ice processes such as the concentration effect or abiotic reactions [*Carpenter et al.* 2005].

-------------------------------------------------------------------------------------------------------------------------

Table 2. Average (Ave) and maximum (Max) halocarbon concentrations (pM) measured in sea ice brine during this study (A), by *Atkinson et al.* [2012] in the Weddell Sea in February 2009 (W), and by *Fogelqvist and Tanhua* [1995] in the Weddell Sea in January and February 1993 (F).

|         | $CH_3I$ | $C_2H_5I$ | $CHBr_3$ | $CH_2ICl$ | $2\text{-}C_3H_7I$ | $CH_2IBr$ | $1\text{-}C_3H_7I$ | $CH_2Br_2$ |
|---------|------|------|------|------|------|------|------|------|
| Ave (A) | 31   | 28   | 128  | 2.1  | 5.6  | 2.8  | 4.8  | 172  |
| Max (A) | 145  | 225  | 593  | 15   | 26   | 26   | 30   | 573  |
| Ave (W) | 5.7  | 30   | 351  | 16   | 16   | 9.4  | 14   | 39   |
| Max (W) | 149  | 739  | 6850 | 455  | 311  | 406  | 258  | 1270 |
| Ave (F) | 38   | 27   | 22   |      | 7.1  |      | 235  |      |
| Max (F) | 41   | 26   | 23   |      |      |      | 259  |      |

-------------------------------------------------------------------------------------------------------------------------

Figure 6 shows halocarbon profiles through the full depth of the water column at the ice station. Profiles of $C_2H_5I$, and $C_3H_7I$ show a strong peak at 10 m, just above the mixed layer depth at 12 m. Previous measurements [*Hughes et al.* 2008] have shown these halocarbons can be produced in marine aggregates which are likely to collect here, as they sink from the upper photic zone due to gravity, but are prevented from sinking further due to the pycnocline barrier. $CH_2Br_2$ is the only halocarbon which shows a similar profile to Chl *a*.
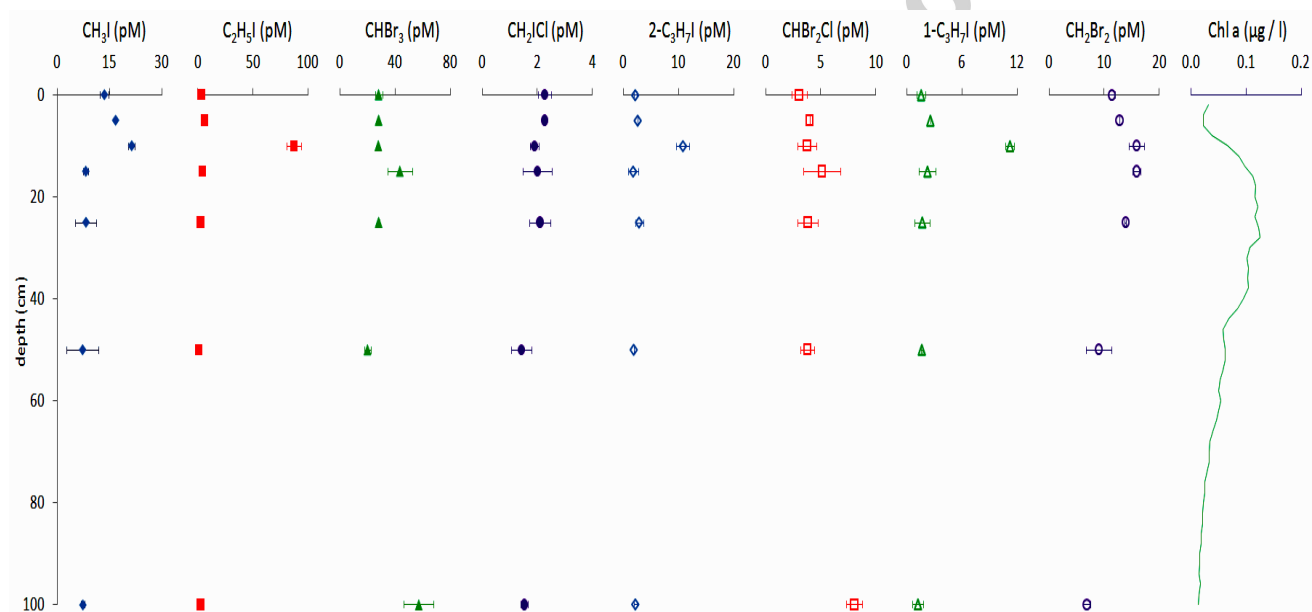


Fig. 6. Halocarbon concentrations through the full depth of CTD water samples whilst at the ice station on 28 June.

As can be seen from the Chl *a* concentrations in Figure 5, the most biologically productive waters were west of Svalbard, and the ice edge algae bloom in this region is clearly seen in the satellite image in Figure S3. The four types of waters in which CTD casts were made are shown in Figure 7. $CH_3I$ and $C_2H_5I$ concentrations are variable and values overlap across all water masses. Concentrations of the iodopropanes are higher in water close to the ice, and $CH_2ICl$ has higher concentration in the deeper water of station KF4, especially at the DCM.

In the dive samples (Figure 8), the larger concentrations of $CHBr_3$, $CH_2Br_2$ and $CH_3I$ suggest these compounds are released from dead or dying algae draining from the ice. Previous work monitoring production of halocarbons over the life cycle of diatoms has shown that production is greatest during growth, and less during stationary and dying phases [*Moore et al.* 1996], which explains a lower halocarbon ratio between the ice brine and dense algae mats than the cell density ratio. When halocarbon concentrations in the different sample types collected at the ice station are compared (Figure 9), the potential for some halocarbons to be enhanced in sea ice brine is clear, though the range is large and overlaps with the seawater concentrations. Production under the ice, the concentration effect in brine, flushing of brine channels with seawater and fresh ice melt all affect halocarbon concentrations, as do degradation by bacteria and loss to the atmosphere. These processes are discussed further below.

### 3.3 Halocarbons in air

In Figure 10, larger concentrations of halocarbons are observed in air masses whose 24 hour back trajectories (courtesy of NOAA, HYSPLIT model, not shown) mostly show they originated above the sea ice of the Arctic to the north, and concentrations reduce as the ship travelled away from the ice.  The small concentrations of all compounds on 19 June could be due to the air mass having originated over Svalbard (not shown), where halocarbon sources are less likely.

Bromocarbon concentrations are similar to previous measurements by others [*Chuck et al.* 2005, *Class and Ballschmiter* 1987, *Quack and Wallace* 2003].  $CH_3I$ mixing ratios are higher than previous measurements in polar regions (Table S2), but similar to measurements at mid-latitudes close to kelp beds [*Carpenter et al.* 1999]; although there is always the possibility that something went wrong with the CH3I standards, this is unlikely as the same standards were used for the sea water and brine measurements. $C_2H_5I$ and $CH_2ICl$ concentrations are also very large compared to previous measurements.

The large bars in air samples over ice in Figure 10 suggest short-term variation in source strengths in the ice area, probably caused by open leads in the ice leading to a short-lived surge in concentrations in the air mass reaching the ship – such a surge might not be present in all three air samples as they are separated by 15 or 30 minutes.  The variability in the open ocean is consistent with the variability in trajectory directions.
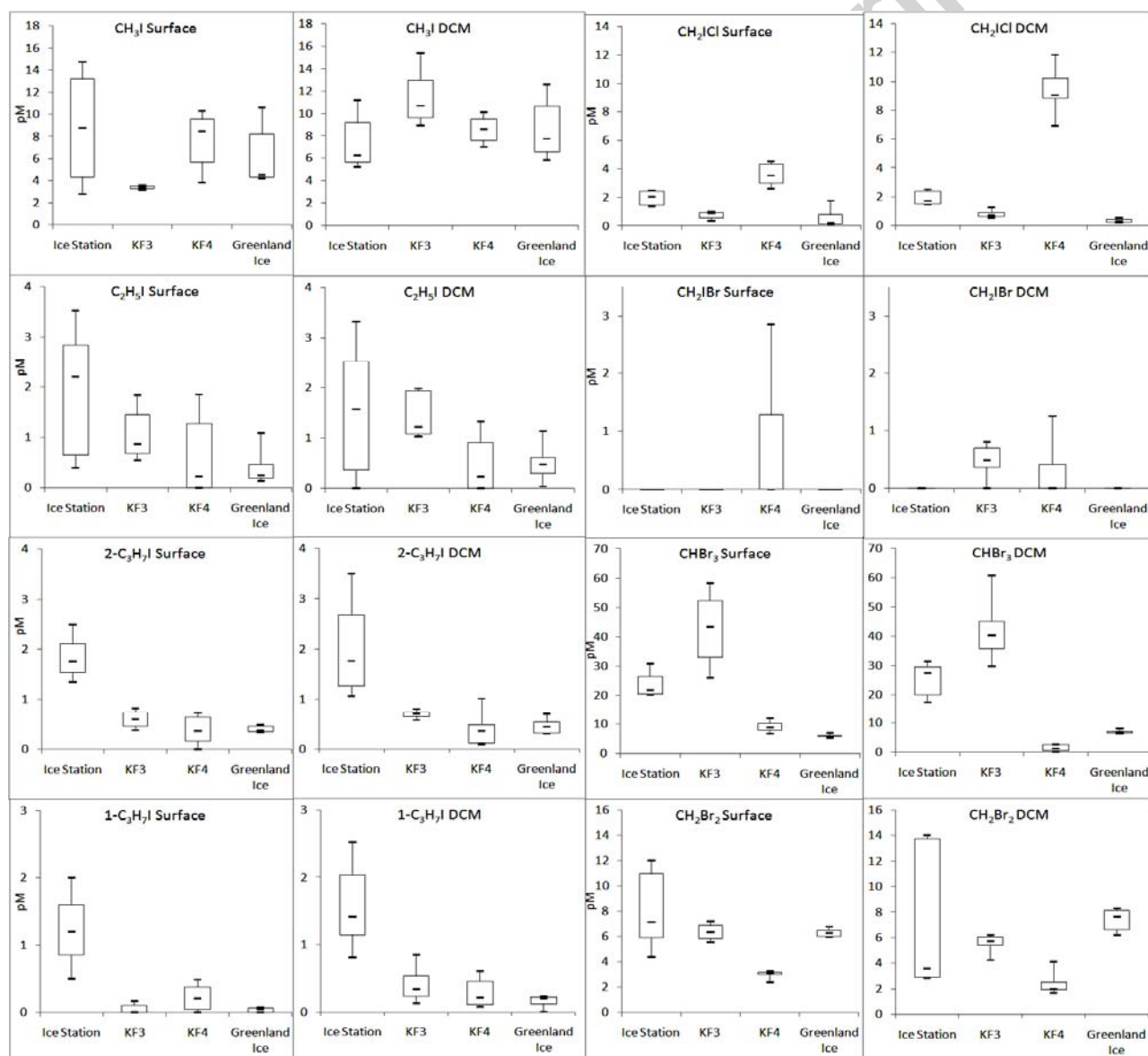


Fig. 7.  Halocarbon concentrations in water samples from CTD casts of different areas: station KF3 is close to Svalbard, and station KF4 is in deeper waters further out to sea.  The boxes are the 20 and 80 percentiles, the dash is the median, and the bars show the maximum and minimum concentrations.
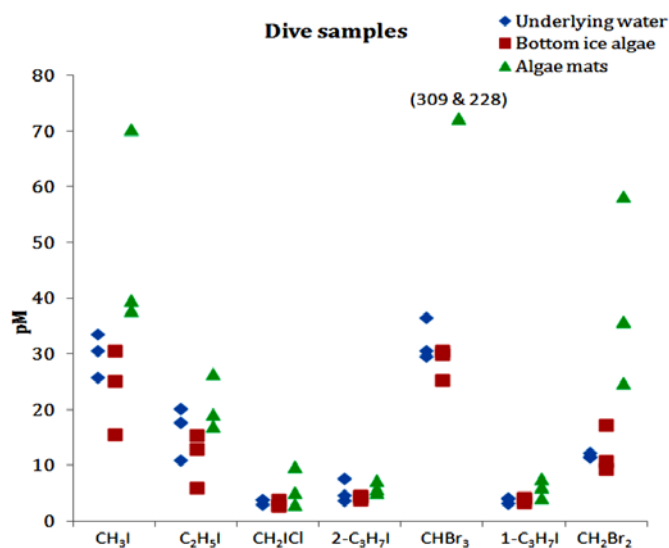
Fig. 8. Halocarbon concentrations in the three types of seawater collected by the dive team. Concentrations of $CHBr_3$ from two algae mat samples are off the scale at 309 and 228 pM.
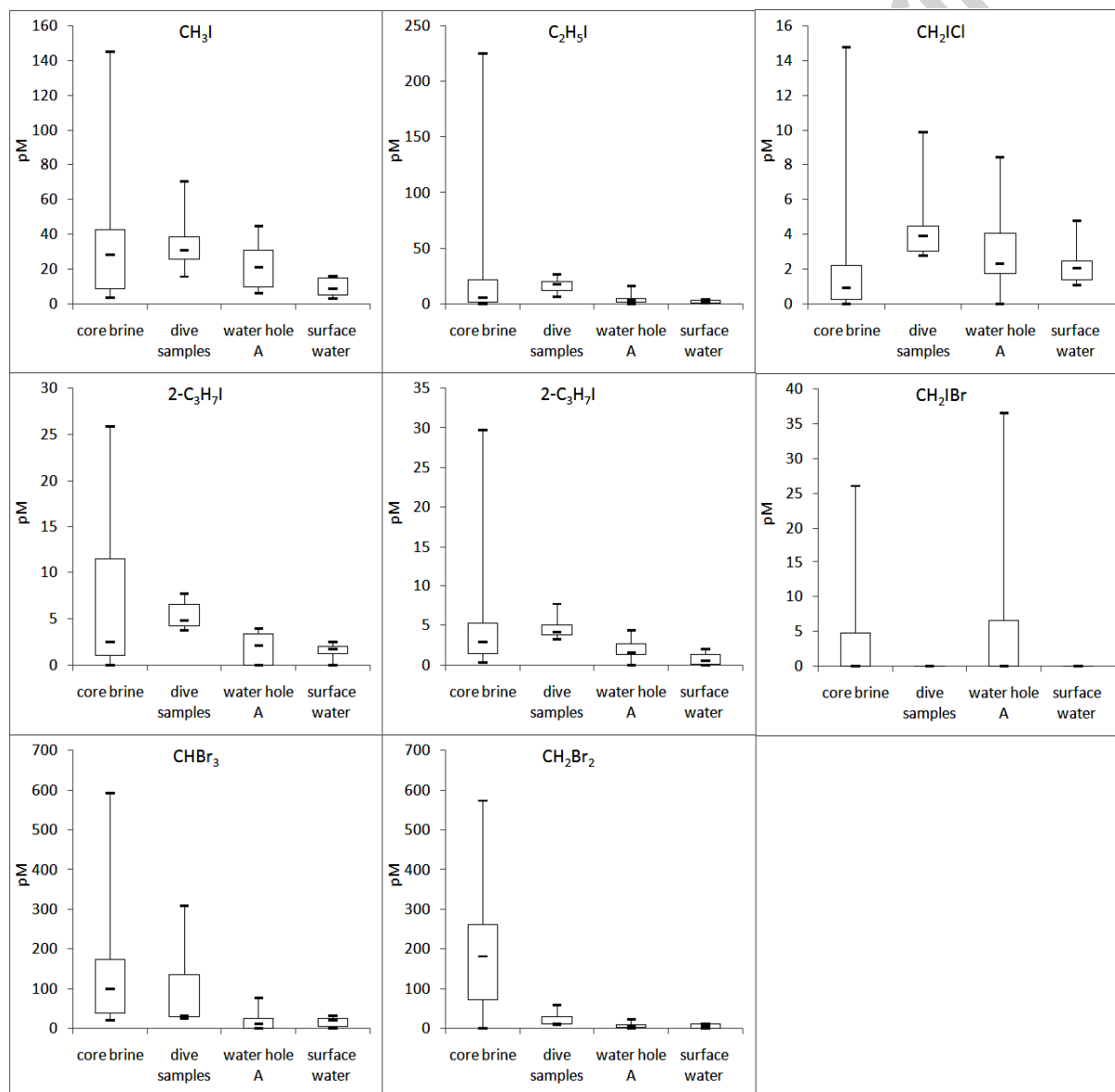


Fig. 9. Summary of water and sea ice brine samples collected at the ice station. The boxes are the 20 and 80 percentiles, the dash is the median, and the bars show the maximum and minimum concentrations.
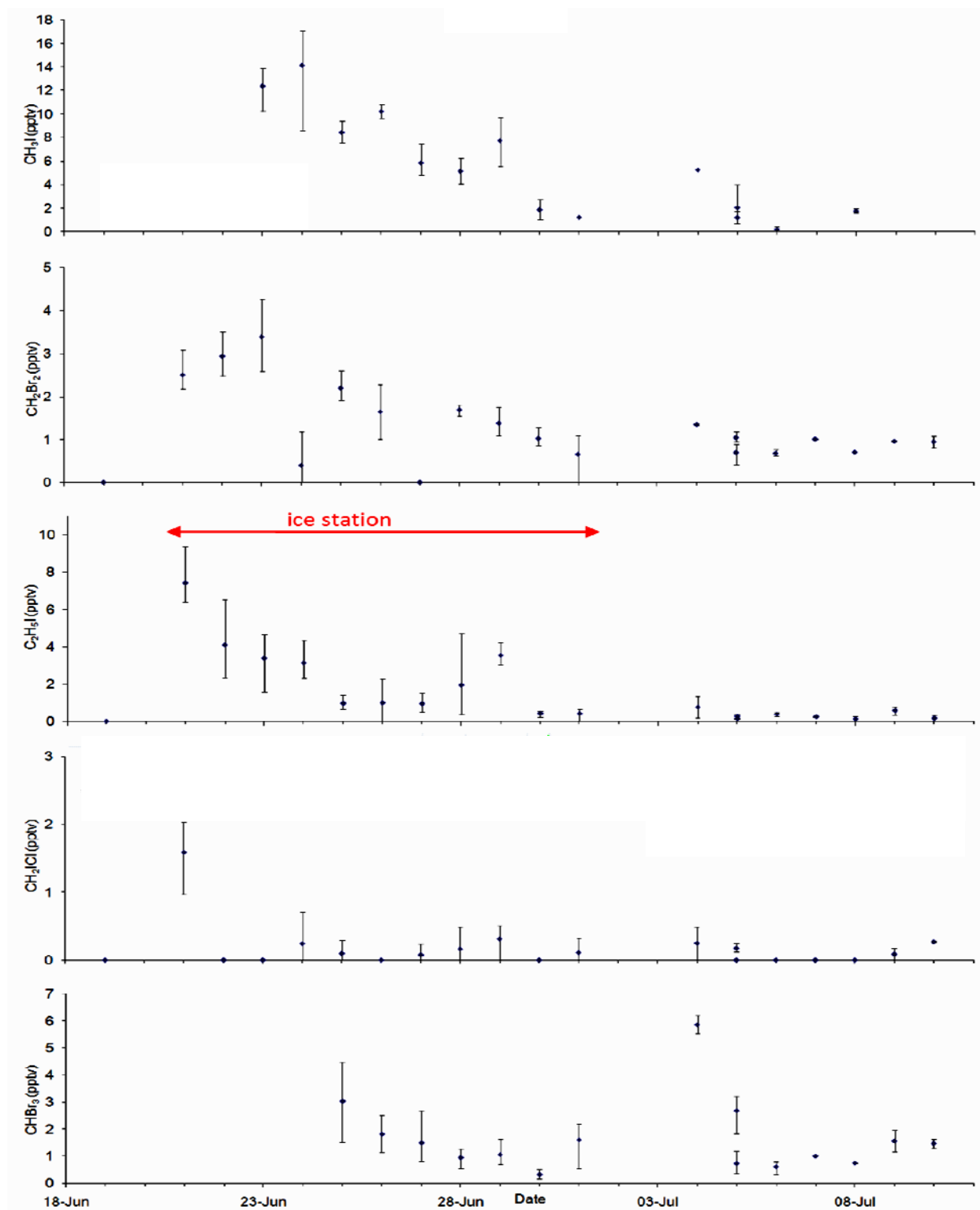
Fig. 10. Atmospheric concentrations of some halocarbons during the campaign. $CH_2IBr$ was only measured above LoD on 21 & 22 June and from 5 to 7 July; 1- and 2-$C_3H_7I$ were below LoD in all samples. CH3I was below LoD on 19, 21 and 22 June; CHBr3 on 19, 21, 22, 23 and 24 June.

### 3.4. Saturation anomalies and flux calculations

Our results show halocarbon concentrations are mostly enhanced in sea ice brine and in under-ice water. Saturation anomalies and fluxes were calculated in order to estimate their importance to regional atmospheric chemistry.

The saturation anomaly is the departure from the expected equilibrium between the concentration in water and the atmosphere. Anomalies were calculated via Equation 3 (Sander [1999]), where $C_w$ is the seawater concentration, $C_a$ is the atmospheric concentration, and $H$ is the temperature dependent Henry's law constant:

Saturation anomaly (%) = 100 x $(C_w–C_a/H)/(C_a/H)$        (3)

In Table 3, $CH_3I$ and $C_2H_5I$ are always supersaturated in surface waters, leading to a flux from ocean to atmosphere, so unsurprisingly they have the highest concentrations in air in Figure 10. $CHBr_3$, $CH_2ICl$ and $CH_2Br_2$ are predominantly supersaturated in surface water, though occasional undersaturation occurs when they may be deposited to the ocean. Saturation anomalies in under-ice water helps assess if they would change the fluxes of halocarbons once these waters were exposed to the atmosphere at the ice edge – possible because currents underneath the ice were as large as 10 cm s$^{-1}$ (Gavin Turner, private communication). The results show some larger anomalies in under-ice than surface water.

Flux calculations followed *Johnson* [2010]. Briefly, the equation $F = K_w(C_a/H – C_w)$ was used, where $F$ is the flux, $K_w$ is the transfer velocity, $C_a$ is the air concentration, $C_w$ the simultaneous water concentration, and $H$ the Henry's law constant as above. Transfer velocities are dependent on wind speed, salinity and water temperature, with wind being a surrogate for the effect of waves and bubbles on gas exchange rates; 7-day average wind speeds were used, together with near-simultaneous concentrations in air and surface water samples. At the ice station, under-ice water concentrations were used in order to calculate the flux at the ice edge when these waters were exposed to the atmosphere.

-------------------------------------------------------------------------------------------------------------------------

Table 3. Saturation anomalies (%) based on simultaneous concentrations in air and surface water ($F_w$) or under-ice water ($F_i$). $CH_2IBr$ 1- and 2-$C_3H_7I$ concentrations were not measured above the LoD in enough air samples for $F_w$ to be calculated.

| | $CH_3I$ | $C_2H_5I$ | $CHBr_3$ | $CH_2ICl$ | $CH_2Br_2$ |
|---|---|---|---|---|---|
| Ave $F_w$ | 1290 | 869 | 143 | 355 | 107 |
| (min-max) | (136-2198) | (28-2528) | (-39-334) | (-60-753) | (-10-203) |
| Ave $F_i$ | 1845 | 656 | 186 | 585 | 51 |
| (min-max) | (391-4698) | (-93-1902) | (9-422) | (426-745) | (8-109) |

-------------------------------------------------------------------------------------------------------------------------

Fluxes from the ice to the atmosphere were also calculated, using halocarbon concentrations in the uppermost sections of the ice cores. This assumes that the concentrations in the brine channels in these upper sections are representative of the concentrations in the liquid film on the ice surface, i.e. that the brine channels are connected and brine migration transports dissolved ions and trace gases to the ice-atmosphere interface. This also assumes that fluxes from a brine layer on the surface of sea ice are analogous to fluxes from the surface microlayer of seawater, an unsubstantiated assumption.

The results in Figure 11 show how fluxes from ocean to atmosphere would generally be larger if waters underneath the ice were transported to the ice edge, and fluxes from sea ice to the atmosphere should be larger still. These results may explain why atmospheric concentrations are larger in Figure 10 in air which has travelled over sea ice.

### 3.5. Fluxes from the ice to the water below

When sea ice forms, salts are expelled from the growing ice to brine channels, eventually draining from the ice. In summer when the ice starts to melt, freshwater dilutes this brine, eventually making it less saline than the seawater underneath. When this point is reached, brine no longer drains by gravity from the channels and a stratified regime takes over. From this point onwards, solute exchange is controlled by molecular diffusion [*Tison et al.* 2010].

From the ice core data in Figure 3, it would appear that a concentration gradient exists in the core of 29 June (right panel) for all compounds except $CH_2ICl$ and $CH_2IBr$. This would result in fluxes from the higher concentrations within the centre of the core to the lower concentrations in the underlying seawater, controlled by molecular diffusion and driven by the concentration gradient. Hence the concentration gradient in these cores, and the molecular diffusion coefficient of seawater at 0°C ($1 \times 10^{-9}$ m$^2$ s$^{-1}$, *Yuan-Hui and Gregory* 1974) were used to calculate fluxes via the brine channels. From Fick's first law of diffusion, flux = $–D(\delta C/\delta t)$, where $(\delta C/\delta t)$ is the concentration gradient and D is the diffusion coefficient. The results range from $9 \times 10^{-8}$ to $8 \times 10^{-6}$ nmol m$^{-2}$ day$^{-1}$, very small values. Therefore

we expect that after brine drainage is complete, halocarbon concentrations initially stay essentially constant in the ice.  Later, as ice melt reduces concentrations in the lower part of the ice, we find by multiplying by brine volume and the average rate of ice melt (3 cm day-1) that fluxes range from 0.003 to 2.4 nmol m$^{-2}$ day$^{-1}$, much larger.
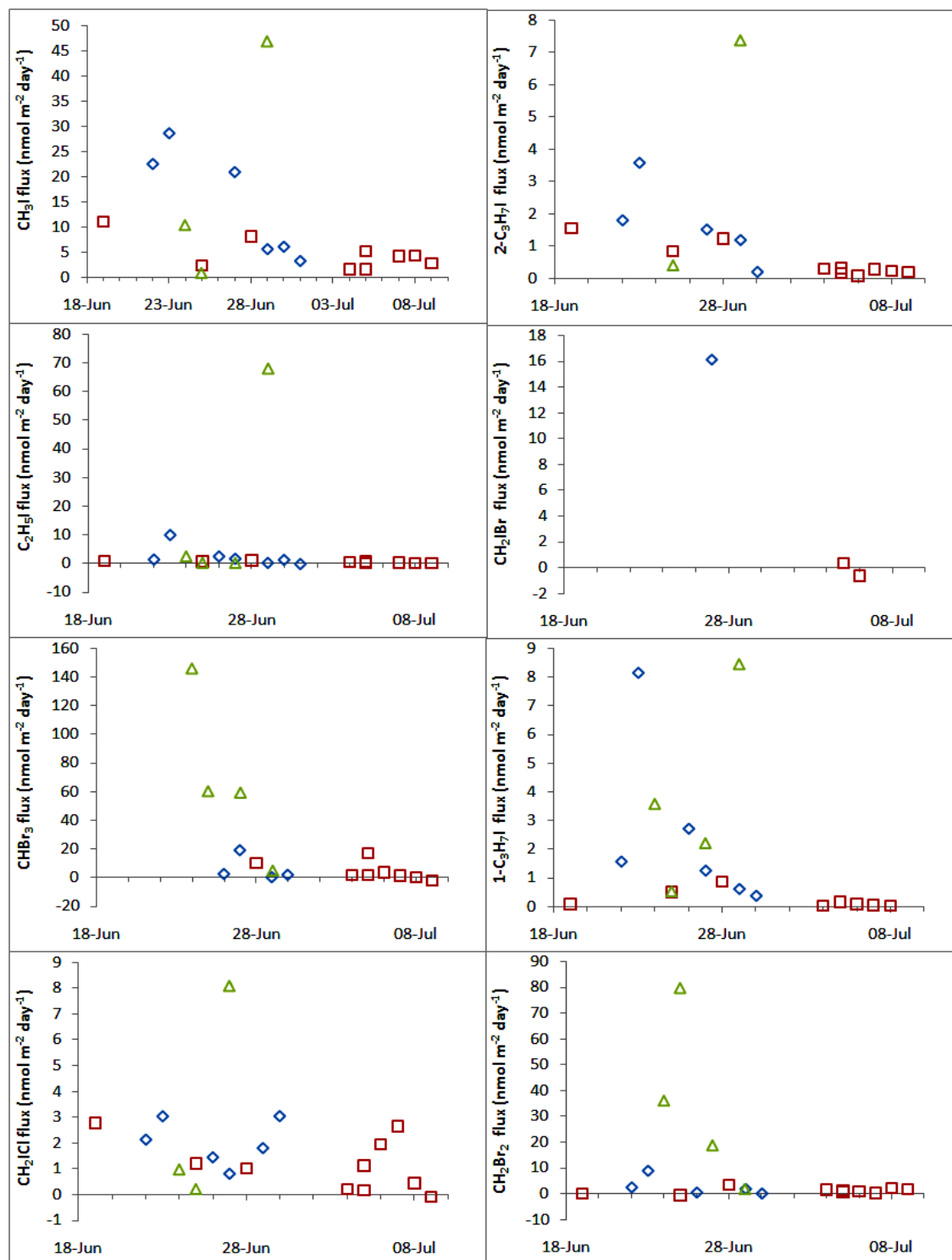


Fig. 11.  Flux estimates (nmol m$^{-2}$ day$^{-1}$) of halocarbons using air concentrations, and same day concentrations in under-ice water (blue diamonds), surface seawater (red squares) and uppermost ice core brine (green triangles).

We also calculated fluxes from the concentration gradients in seawater near the hole in the ice, using the gradient as a function of the distance of the sampling tube from the ice interface, whilst this distance increased with time. These fluxes should also include contributions from production by the bottom-of-ice and under-ice water communities, so the difference from the above brine-channel calculation should reflect *in-situ* production.  This is an approximation as horizontal and vertical water currents have not been considered, but a stratified water column was observed during the depth profile of the 28 June so vertical exchange is arguably minimal.  The resultant production under the ice is

0.2, 0.06, 0.9, 0.004, 0.02, 0.03, 0.02 and 2.4 nmol m$^{-2}$ day$^{-1}$ for $CH_3I$, $C_2H_5I$, $CHBr_3$, $CH_2ICl$, 2-$C_3H_7I$, $CH_2IBr$, 1-$C_3H_7I$ and $CH_2Br_2$ respectively.

### 3.6. Discussion of halocarbon concentrations and fluxes in Arctic summer

A complex system affects halocarbon concentrations, including production by diatoms [*Sturges et al.* 1992], uptake by bacteria [*Goodwin et al.* 1997, *Goodwin et al.* 1998], and fluxes between the ice, air and atmosphere. Results from the ice cores show how concentrations are enhanced in sea ice brine, and enhanced concentrations in under-ice water samples show how the under-ice bloom may also produce halocarbons. In order to estimate the contribution of these processes, the various production and loss processes have been considered, as illustrated in Figure 12.

Fi and Fw have been calculated in Sections 3.4 and 3.5, plus contributions from the under-ice algae. Assuming similar factors affect fluxes from a liquid brine layer on the surface of sea ice, ice-atmosphere fluxes have the potential for a greater contribution to the atmospheric halogen budget than fluxes from open water, and the flux at the ice edge due to waters influenced by under-ice communities may be similar.

How other factors affect fluxes from the ice surface are not known, for example the effect of a snow layer. One might think snow would suppress fluxes, but it is very porous, and very cold temperatures may in fact increase halogen reactivity [*Cho et al.* 2002]. The presence of halogen radicals or ions in the quasi-liquid layer in snow may make them more available for reaction due to their highly polarisable nature, more so for the large iodide ion.
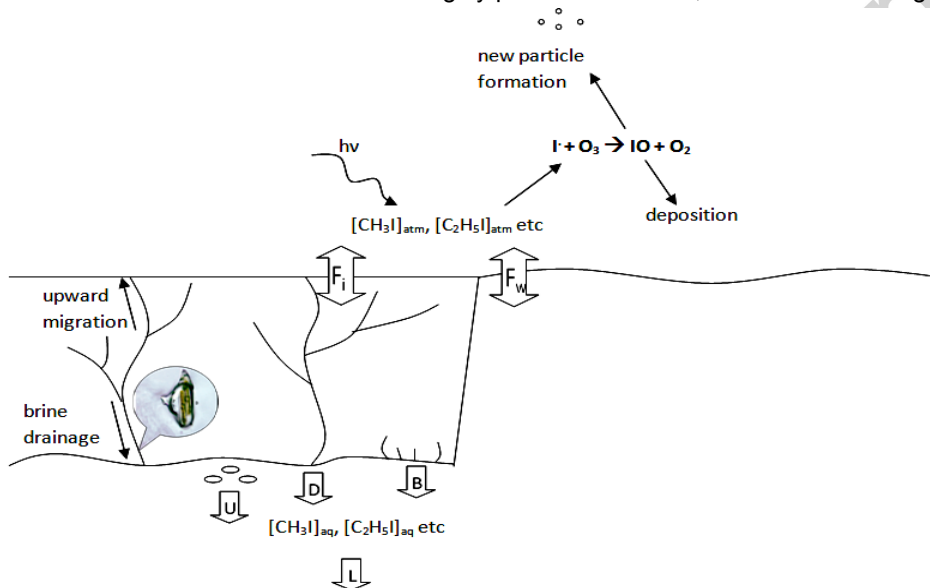


Fig. 12. Processes contributing to halocarbon concentrations. Fi and Fw are ice- and water-atmosphere fluxes, U is production by under-ice diatoms, D is brine channel drainage, B is production by the bottom ice community, and L is loss to the underlying seawater and other processes discussed in the text.

The largest halocarbon flux to the water underneath the ice is from ice melt and under-ice diatom production, whereas brine channel drainage contributes little under summer conditions. The reasons for halocarbon production have not been conclusively determined, but one possibility is in response to grazing [*Manley* 2002], and enhanced halocarbon concentrations in brine channels may occur as ice melts and brine channels widen, allowing small zooplankton to enter and grazing pressure on the ice communities to increase.

### 3.7. Correlations between halocarbon concentrations

Correlation plots were made of the concentration of one halocarbon versus another, for all the samples of sea ice brine. This was repeated for all possible pairs of halocarbons. Significant correlations were found between $CH_3I$ and $C_2H_5I$, and between CH3I or $C_2H_5I$ and 1- or 2-$C_3H_7I$ ($R^2$ values 0.76 to 0.94). The process was repeated for all water samples, where correlations were found between the same halocarbons but with smaller $R^2$ (0.42 to 0.62). We found no correlations between bromocarbons, in contrast to *Schall et al.* [1997] who showed a correlation between $CHBr_3$ and $CH_2Br_2$.

Others have noted poor correlation between bromocarbons close to sources [*Carpenter and Liss* 2000, *Hughes et al.* 2009]. *Schall et al.* [1997] found that bromocarbon concentrations were linked to Chl *a* but iodocarbons were not, but we only found a correlation between Chl *a* and $CH_2ICl$. One difficulty is that Chl *a* is not necessarily a reliable indication of total biomass as different species fluoresce by different amounts, and halocarbon production is also species dependent. The picture is further complicated in ice, as when the brine drains the diatoms remain stuck to the walls of the brine channels [*Krembs et al.* 2002].

### 3.8. The sub-Arctic in early spring

Results from this earlier campaign are discussed in Supplementary Material S2. Briefly, in the more saline core, $C_2H_5I$ and $CHBr_3$ have similar profiles with surface enhancement, which could be due to expelled brine, or surface flooding due to tidal cracks because of nearby land; $CH_2I_2$ and $CH_2IBr$ have similar profiles, implying a common source; and the concentration of $CH_2IBr$ is surprisingly large. This is an interesting result as this was the most abundant iodocarbon in the atmosphere in the earlier campaign in the same location [*Carpenter et al,* 2005]. Halocarbons were detected in air masses which had passed over open water, and IO was up to 3.4 pptv in the same air masses. This suggests that halocarbons are trapped in the ice, and may only escape when the ice is melting or when leads open in the ice.

Using the maximum rate of ice melt in Hudson Bay [*Wang et al.* 1994] and our maximum halocarbon concentrations, fluxes of $CH_3I$, $C_2H_5I$, $CHBr_3$, $CH_2IBr$, $1-C_3H_7I$ and $CH_2Br_2$ to the air during later ice melt could be as high as 4.3, 1.2, 1.0, 0.7, 0.4 and 0.3 $nmol\,m^{-2}\,day^{-1}$. These values are similar to those calculated above for the Arctic summer.

### 4. Conclusion

Average halocarbon concentrations in sea ice brine in the Arctic in summer were 31, 28, 128, 2.1, 5.6, 2.8, 4.8 and 172 pM for $CH_3I$, $C_2H_5I$, $CHBr_3$, $CH_2ICl$, $2-C_3H_7I$, $CH_2IBr$, $1-C_3H_7I$ and $CH_2Br_2$, respectively. The ice was very warm and very porous, and the high concentrations of halocarbons in the brine of the sea ice, despite its large porosity, suggest a local source. One possibility is the concentration effect of brine volume reduction. Another is production by enzymes in organisms which make up the sea ice community, which may be particularly active in the harsh environment experienced in the brine channels. Halocarbon production may also be related to defence in response to grazing [*Manley* 2002], so enhanced halocarbon concentrations in brine channels may occur as ice melts and brine channels widen, allowing zooplankton to enter and grazing pressure on the ice communities to increase.

Flux calculations using simultaneous halocarbon concentrations in sea-water or ice brine and concentrations in air show the potential for enhanced fluxes from the sea ice, but major assumptions have been made about factors affecting the fluxes, such as the lack of an effect due to snow cover, and there is debate about the correct methodology for such calculations. However, waters reaching the ice edge from under-ice communities may supply a flux of similarly large magnitude to those we calculate from the sea ice brine. Estimates of halocarbon fluxes from the sea ice to the water below suggest the largest contribution is from ice melt and under-ice diatom production - brine channels contribute little under summer conditions.

The halocarbon concentrations in Arctic summer were similar to those in sea ice with similar physical properties in the Antarctic during late summer [*Atkinson et al. 2012*]. The water below the ice in the Antarctic also showed high halocarbon concentrations, due to ice melt and production by underwater diatoms. $1-C_3H_7I$, $CHBr_3$, $C_2H_5I$, $2-C_3H_7I$, and $CH_2Br_2$ showed significant enhancement in concentration in the Arctic brine, relative to sea water, of order 2.5, 3, 7, 7, and 23 times respectively. After normalising to brine volume, the average enhancements factors of $C_2H_5I$, $2-C_3H_7I$ and $CH_2Br_2$ were 1.7, 1.4 and 2.5 times respectively.

The ice properties in Arctic summer were quite different from those in our sub-Arctic campaign: the ice in the Arctic in summer was about 1 m thick and very porous, whereas the ice in the sub-Arctic in early spring was thicker, colder and less porous. These different ice properties enabled a further investigation of the concentration effect, and higher concentrations of halocarbons were found in the brine of the spring ice despite much lower algal activity. The measurements in spring suggest that the halocarbons, concentrated much more by brine volume reduction in the colder temperatures, remain trapped in the colder ice because brine channels are not interconnected. Diffusion through sea ice is too slow for release of halocarbons to the atmosphere, and *Mahajan et al.* [2010] suggest it arises when leads open in the ice.

In the Arctic in summer, very high atmospheric concentrations of halocarbons were measured, for some compounds the highest ever recorded. They were especially high at the ice station, when the wind was mainly from the north,

thereby traversing sea ice, which was very porous at the time. Although transport of gases through solid ice is negligible, halocarbon transport through the bulk ice may be large under these conditions.

The concentrations in Arctic ice were similar to those measured in the Antarctic, suggesting similar processes involving organic halogens associated with sea ice in both polar regions. But in the Antarctic, atmospheric IO concentrations were similar to those of BrO, whereas IO concentrations were much lower in the Arctic. This could be due to the larger proportion of thinner ice in the Antarctic that becomes porous or melts in summer - porous ice has additional space for algal colonisation, thinner ice lets more light penetrate to under-ice diatoms.

As the Arctic warms during the 21st Century, and the ice becomes thinner and more porous, the potential for trace gases dissolved in the brine to be released to the atmosphere above is greater. In particular, there is increased potential for iodocarbons to be released from the ice and for iodine compounds in general to be transported from ocean to atmosphere. The resultant increase in iodine radicals in the troposphere would have important implications for tropospheric ozone loss, oxidising capacity and new particle formation.

**References**
Arrigo, K. R., and D. N. Thomas (2004), Large scale importance of sea ice biology in the Southern Ocean, in *Antarctic Science*, edited, pp. 471-486.

Atkinson, H.M., R-J. Huang, R. Chance, H.K. Roscoe, C. Hughes, B. Davison, A. Schönhardt, A. S. Mahajan, A. Saiz-Lopez, P.S. Liss, "Iodine Emissions from the sea ice of the Weddell Sea", *Atm. Phys. Chem.* **12**, 11229–11244, doi:10.5194/acp-12-11229-2012, (2012).

Bari, S., and J. Hallett (1974), Nucleation and growth of bubbles at an ice-water interface.

Carpenter, L. J., and P. S. Liss (2000), On temperate sources of bromoform and other reactive organic bromine gases, *J. Geophys. Res.*, *105*(D16), 20539-20547.

Carpenter, L. J., D. J. Wevill, C. J. Palmer, and J. Michels (2007), Depth profiles of volatile iodine and bromine-containing halocarbons in coastal Antarctic waters, *Marine Chemistry*, *103*(3-4), 227-236.

Carpenter, L. J., J. R. Hopkins, C. E. Jones, A. C. Lewis, R. Parthipan, D. J. Wevill, L. Poissant, M. Pilote, and P. Constant (2005), Abiotic Source of Reactive Organic Halogens in the Sub-Arctic Atmosphere?, in *Environmental Science and Technology*, edited, pp. 8812-8816.

Chameides, W. L., and D. D. Davis (1980), Iodine- Its possible role in tropospheric photochemistry, in *Journal of Geophysical Research*, edited, pp. 7383-7398.

Class, T., and K. Ballschmiter (1987), Chemistry of organic traces in air IX: Evidence of natural marine sources for chloroform in regions of high primary production, *Fresenius' Journal of Analytical Chemistry*, *327*(1), 40-41.

Cox, G., and W. Weeks (1983), Equations for determining the gas and brine volumes in sea-ice samples, *Journal of Claciology*, *29*(102), 306-316.

Davis, D., J. Crawford, S. Liu, S. McKeen, A. Bandy, D. Thornton, F. Rowland, and D. Blake (1996), Potential impact of iodine on tropospheric levels of ozone and other critical oxidants, in *Journal of Geophysical Research*, edited, pp. 2135-2147.

Dyrssen, D., and E. Fogelqvist (1981), Bromoform concentrations of the Arctic Ocean in the Svalbard area, *Oceanol. Acta*, *4*, 313-317.

Fogelqvist (1985), CARBON TETRACHLORIDE. TETRACHLOROETHYLENE, 1,1,1-TRICHLOROETHANE AND BROMOFORM IN ARCTIC SEAWATER, *J. Geophys. Res.*, *90*(C5), 9181-9193.

Fogelqvist, and M. Krysell (1991), Naturally and anthropogenicaly produced bromoform in the Kattegatt, a semi-enclosed oceanic basin, *Journal of Atmospheric Chemistry*, *13*(4), 315-324.

Fogelqvist, and T. Tanhua (1995), Iodinated C1-C4 hydrocarbons released from ice algae in Antarctic, *Naturally Produced Organohalogens*, 295-307.

Frankenstein, G., and R. Garner (1967), Equations for determining the brine volume of sea ice from-0.5 C to-22.9 C, *Journal of Glaciology*, *6*, 943-944.

Garrison, D. L., and K. R. Buck (1989), The biota of Antarctic pack ice in the Weddell sea and Antarctic Peninsula regions, *Polar Biology*, *10*(3), 211-219.

Golden, K., S. Ackley, and V. Lytle (1998), The percolation phase transition in sea ice, *Science*, *282*(5397), 2238.

Gosink, T. A., J. G. Pearson, and J. J. Kelley (1976), Gas movement through sea ice.

Haas, C., D. N. Thomas, and J. Bareiss (2001), Surface properties and processes of perennial Antarctic sea ice in summer, *Journal of Glaciology*, *47*(159), 613-625.

Happell, J. D., and D. W. R. Wallace (1996), Methyl iodide in the Greenland/Norwegian Seas and the tropical Atlantic Ocean: Evidence for photochemical production, *Geophys. Res. Lett.*, *23*(16), 2105-2108.

Hemmingsen, E. (1959), Permeation of gases through ice, *Tellus*, *11*(3), 355-359.

Horner, R., S. F. Ackley, G. S. Dieckmann, B. Gulliksen, T. Hoshiai, L. Legendre, I. A. Melnikov, W. S. Reeburgh, M. Spindler, and C. W. Sullivan (1992), Ecology of sea ice biota. I: Habitat, terminology, and methodology, edited, pp. 417-427, Springer.

Hughes, C., G. Malin, C. Turley, B. Keely, P. Nightingale, and P. Liss (2008), The production of volatile iodocarbons by biogenic marine aggregates, Limnology and Oceanography, 53(2), 867-872.

Hughes, C., A. L. Chuck, H. Rossetti, P. J. Mann, S. M. Turner, A. Clarke, R. Chance, and P. S. Liss (2009), Seasonal cycle of seawater bromoform and dibromomethane concentrations in a coastal bay on the western Antarctic Peninsula, *Global Biogeochemical Cycles*, *23*(2), GB2024.

Johnson, M. (2010), A numerical scheme to calculate temperature and salinity dependent air-water transfer velocities for any gas, *Ocean Sci*, *6*, 913–932.

Jones, C. E., and L. J. Carpenter (2005), Solar photolysis of CH2I2, CH2ICl, and CH2IBr in water, saltwater, and seawater, *Environmental science & technology*, *39*(16), 6130-6137.

Krembs, C., H. Eicken, K. Junge, and J. Deming (2002), High concentrations of exopolymeric substances in Arctic winter sea ice: implications for the polar ocean carbon cycle and cryoprotection of diatoms, *Deep Sea Research Part I: Oceanographic Research Papers*, *49*(12), 2163-2181.

Loose, B., P. Schlosser, D. Perovich, D. Ringelberg, D. Ho, T. Takahashi, J. RICHTER MENGE, C. Reynolds, W. McGillis, and J. L. TISON (2011), Gas diffusion through columnar laboratory sea ice: implications for mixed layer ventilation of CO2 in the seasonal ice zone, *Tellus B*.

Mahajan, A. S., M. Shaw, H. Oetjen, K. E. Hornsby, L. J. Carpenter, L. Kaleschke, X. Tian-Kunze, J. D. Lee, S. J. Moller, and P. Edwards (2010), Evidence of reactive iodine chemistry in the Arctic boundary layer, *Journal of Geophysical Research*, *115*(D20), D20303.

Manley, S. L. (2002), Phytogenesis of halomethanes: A product of selection or a metabolic accident?, edited, pp. 163-180, Springer.

Moore, M. Webb, R. Tokarczyk, and R. Wever (1996), Bromoperoxidase and iodoperoxidase enzymes and production of halogenated methanes in marine diatom cultures, in *JGR*, edited, pp. 20899-20908, AGU.

Moore, R., and R. Tokarczyk (1993), Volatile biogenic halocarbons in the northwest Atlantic, *Global Biogeochemical Cycles*, *7*(1), 195-210.

Moore, R. M., and W. Groszko (1999), Methyl iodide distribution in the ocean and fluxes to the atmosphere, *Journal of Geophysical Research*, *104*(C5), 11.163–111.171.

O'Dowd, C. D., J. L. Jimenez, R. Bahreini, R. C. Flagan, J. H. Seinfeld, K. Hameri, L. Pirjola, M. Kulmala, S. G. Jennings, and T. Hoffmann (2002), Marine aerosol formation from biogenic iodine emissions, *Nature*, *417*(6889), 632-636.

Rasmussen, R., M. Khalil, R. Gunawardena, and S. Hoyt (1982), Atmospheric methyl iodide (CH3I), *Journal of Geophysical Research*, *87*(C4), 3086-3090.

Saiz-Lopez, A., A. S. Mahajan, R. A. Salmon, S. J. B. Bauguitte, A. E. Jones, H. K. Roscoe, and J. M. C. Plane (2007), Boundary Layer Halogens in Coastal Antarctica, edited, p. 348, AAAS.

Sander, R. (1999), Compilation of Henry's law constants for inorganic and organic species of potential importance in environmental chemistry, edited, Max-Planck Institute of Chemistry, Air Chemistry Dept.

Schall, C., and K. G. Heumann (1993), GC determination of volatile organoiodine and organobromine compounds in Arctic seawater and air samples, *Fresenius' Journal of Analytical Chemistry*, *346*(6), 717-722.

Schall, C., K. Heumann, and G. Kirst (1997), Biogenic volatile organoiodine and organobromine hydrocarbons in the Atlantic Ocean from 42 N to 72 S, *Fresenius' Journal of Analytical Chemistry*, *359*(3), 298-305.

Schoenhardt, A., A. Richter, F. Wittrock, H. Kirk, H. Oetjen, H. K. Roscoe, and J. P. Burrows (2008), Observations of iodine monoxide columns from satellite, *Atmos. Chem. Phys.*, *8*(3), 637-653.

Slingo, A. (1990), Sensitivity of the Earth's radiation budget to changes in low clouds, *Nature*, *343*(6253), 49-51.

Spindler, M. (1990), A comparison of Arctic and Antarctic sea ice and the effects of different properties on sea ice biota, *Geological history of the Polar Oceans: Arctic Versus Antarctic. Kluwers Academis Publishers*, 173-186.

Strickland, J., and T. Parsons (1968), A practical handbook of seawater analysis, *Bull. Fish. Res. Bd. Can*, *167*, 311.

Sturges, W. T., G. F. Cota, and P. T. Buckley (1992), Bromoform emission from Arctic ice algae, *Nature*, *358*(6388), 660-662.

Swanson, A. L., N. J. Blake, J. E. Dibb, M. R. Albert, D. R. Blake, and F. Sherwood Rowland (2002), Photochemically induced production of CH3Br, CH3I, C2H5I, ethene, and propene within surface snow at Summit, Greenland, *Atmospheric Environment*, *36*(15-16), 2671-2682.

Tison, J. L., F. Brabant, I. Dumont, and J. Stefels (2010), High-resolution dimethyl sulfide and dimethylsulfoniopropionate time series profiles in decaying summer first-year sea ice at Ice Station Polarstern, western Weddell Sea, Antarctica, *J. Geophys. Res.*, *115*(G4), G04044.

Tokarczyk, R., and R. M. Moore (1994), Production of volatile organohalogens by phytoplankton cultures, *Geographical Research Letters*, *21*(4), 285-288.

Wang, J., L. A. Mysak, and R. G. Ingram (1994), A Numerical Simulation of Sea Ice Cover in Hudson Bay, *Journal of Physical Oceanography*, *24*(12), 2515-2533.

Welch, H. E., and M. Bergmann (1989), Seasonal development of ice algae and its prediction from environmental factors near Resolute, NWT, Canada, *Canadian journal of fisheries and aquatic sciences*, *46*(10), 1793-1804.

Yokouchi, Y., L. A. Barrie, D. Toom, and H. Akimoto (1996), The seasonal variation of selected natural and anthropogenic halocarbons in the arctic troposphere, *Atmospheric Environment*, *30*(10-11), 1723-1727.

Yuan-Hui, L., and S. Gregory (1974), Diffusion of ions in sea water and in deep-sea sediments, *Geochimica et Cosmochimica Acta*, *38*(5), 703-714.